Simplified UV-preionized long-pulse TEA CO_2-laser amplifier

Kohshichi Nemoto, Sumio Kogoshi, Etsuo Noda, Tadashi Sekiguchi, and Hirokazu Ohhashi

Department of Electrical Engineering, University of Tokyo, Hongo, Bunkyo, Tokyo, Japan 113

(Received 29 December 1983; accepted for publication 12 May 1984)

A simplified UV-preionized long-pulse TEA CO_2-laser amplifier is proposed, which is powered by a common Marx generator for both the preionization arc discharges and the main laser discharge. The measurements of small-signal gain reveal that there exists an optimum capacitance for the capacitors which are provided in the preionization circuit for the control of preionization level. The physical interpretation for this is also given. A small-signal gain higher than 3%/cm and an extraction energy of nearly 14 J/l (at the input energy level of nearly 1 J) have been achieved. It has also been demonstrated that the amplifier can amplify a long laser pulse of the order of microseconds without serious distortion of pulse waveform.

INTRODUCTION

In most high-pressure pulsed gas lasers, various schemes of preionization are employed, such as corona discharges,[1] UV irradiation,[2,3] and electron-beam injection.[4] Among them, the UV-preionization technique is frequently used for a small- or medium-size TEA-pulsed CO_2 laser with a comparatively long laser pulse duration ($\gtrsim 50$ ns) because of its relative simplicity.

This article proposes a further simplified, long-pulse TEA CO_2-laser amplifier with the pulse duration of the order of microseconds. Conventional double-discharge TEA CO_2-laser amplifiers have two separate capacitor banks as energy sources, one for the main discharge and the other for the preionization discharge, together with a timing-control unit between these two sources. The TEA CO_2 laser proposed in this article, on the other hand, is powered by one common Marx generator for both the UV preionizing and main laser discharges. Thus, the provision of one energy source and a timing-control unit becomes unnecessary, and the system becomes simpler with an increase in maintainability. The measurements of small-signal gain reveal that there exists an optimum capacitance value for the capacitors which are provided in the UV preionizing circuit for the control of UV preionization. Theoretical interpretation for this is also presented.

This laser amplifier is a preamplifier stage for a pulsed CO_2-laser system with total output energy of the order of kilojoules and waveform-controllable long-pulse duration of the order of microseconds. This laser system is to be used to produce a large amount of hot plasma particles from a freely falling ice pellet of hydrogen isotope to fill a magnetic container of any given type with clean parameter-controlled laser-produced plasma.[5]

I. EXPERIMENTAL SETUP

The experimental setup is shown in Fig. 1, which consists of an oscillator system and the preamplifier stage which is the main concern of this article. The oscillator system employed is what is called "hybrid type"[6,7] which is the cascade combination of a low-pressure cw CO_2-laser section and a conventional TEA-pulsed CO_2-laser section. This system enables us to obtain a single-longitudinal-mode laser oscillation with a long-pulse duration (of the order of μs), as well as to control the pulse waveform by adjusting the output power of the cw section. This oscillator is utilized to measure the amplification factor of the preamplifier stage concerned.

The preamplifier stage to be tested is a conventional double-discharge UV-excited TEA type, the cross section of which is shown in Fig. 2. A pair of main-discharge electrodes with 76-cm length and 5.5-cm width are machined from an aluminum plate of 1-cm thickness so as to have round edges with a radius of curvature of 2.75 cm at both ends in the axial direction and 1 cm at both edges in the cross section. The gap spacing of the main-discharge electrodes is fixed at 3.5 or 2.5 cm. Two series of arc gaps for preionization (each containing 17 gaps) are provided in parallel on both the top and bottom walls of the container. Thus, the preionization circuit contains 34 arc gaps on each of the container walls, and the gap spacing is nearly 1 mm between the copper electrodes of 2.5-cm length and 1-cm width. The minimum distance between the main-discharge electrodes and these arc-gap electrodes is 4.5 cm, which is found to be sufficient to avoid the occurrence of gas breakdown between them.

A schematic diagram of the power supply circuit is shown in Fig. 3. Both the main and preionization discharges

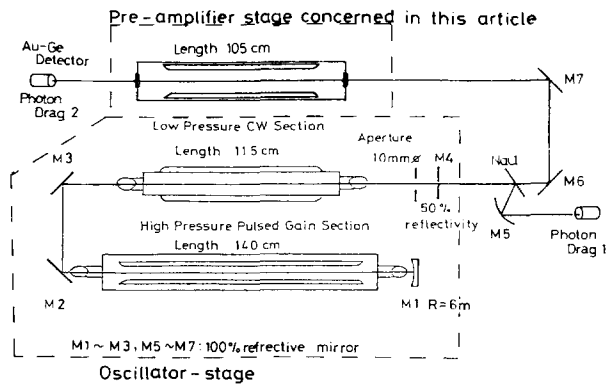

FIG. 1. Experimental setups.

 0034-6748/84/101545-06$01.30 © 1984 American Institute of Physics

Downloaded 13 May 2011 to 10.0.105.126. Redistribution subject to AIP license or copyright; see http://rsi.aip.org/about/rights_and_permissions

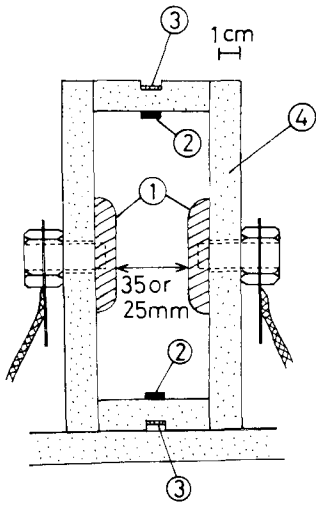

FIG. 2. Cross section of the amplifier to be tested; (1) main electrode (aluminum), (2) arc-gap series for preionization, (3) return circuit for preionization, and (4) container (acrylic plate).

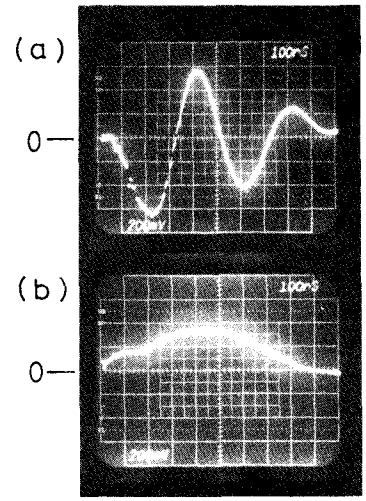

FIG. 4. Current waveform of (a) the preionization current (0.28 kA/div.) and (b) the main-discharge current (5.6 kA/div.); time scale 100 ns/div., electrode spacing $d = 3.5$ cm, Marx charging voltage $V_c = 23$ kV, CO_2:N_2:He = 3:3:8, and $4C_p = 9.6$ nF.

are powered by a common two-stage Marx generator (64-kV erected voltage and 0.108-μF total capacitance). The four capacitors C_p are specially inserted capacitance for controlling the preionization energy.

Total pressure of the working mixture gas (CO_2/N_2/He) is fixed at nearly 1-atm pressure, the gas-flow rate is about 7 l/min, and the concentration ratio is varied. The liquid tri-n-propylamine having lower ionization potential is introduced ($\sim$0.01 cc/l) to the working mixture gas (by using helium as carrier gas) in order to avoid the occurrence of arcing between the main electrodes.

II. EXPERIMENTAL RESULTS

The current waveforms of the main and preionization discharge, which are measured by the combination of Rogowski coils R.C.1 and 2 (Fig. 3) and integrator circuits, are shown in Fig. 4, which confirm that both currents rise simultaneously.

The small-signal gain of the preamplifier concerned is determined by using a 1-w, single-pass, probing cw CO_2-laser beam; Au–Ge photodetector (Fujitsu GC-200-B4); and 7633 Tektronics oscilloscope (Fig. 1). A typical oscilloscope trace of the recorded gain signal is shown in Fig. 5, which indicates that the rise time of the small-signal gain is about 1 μs. It is also observed that duration of the gain signal (FWHM) increases from 2 to 6 μs with increasing relative concentration of nitrogen gas.

The magnitude of small-signal peak gain is found to vary with the capacitance value of the capacitor C_p (Fig. 3), as shown in Fig. 6. The results indicate that there exists an optimum value of $4C_p$ ranging from 10 to 20 nF for each value of the charging voltage (V_c). The same trend is seen also in the case of a smaller electrode spacing of 2.5 cm.

Figures 7(a) and 7(b) show the effect of the relative gas concentration on the peak gain. In Fig. 7(a), the conditions $4C_p = 9.6$ nF and CO_2:N_2 = 1:1 are maintained, and the curves are seen to have their maximum at the abscissa value of 0.35–0.45 [namely, at nearly (CO_2 + N_2):He = 3:4]. In

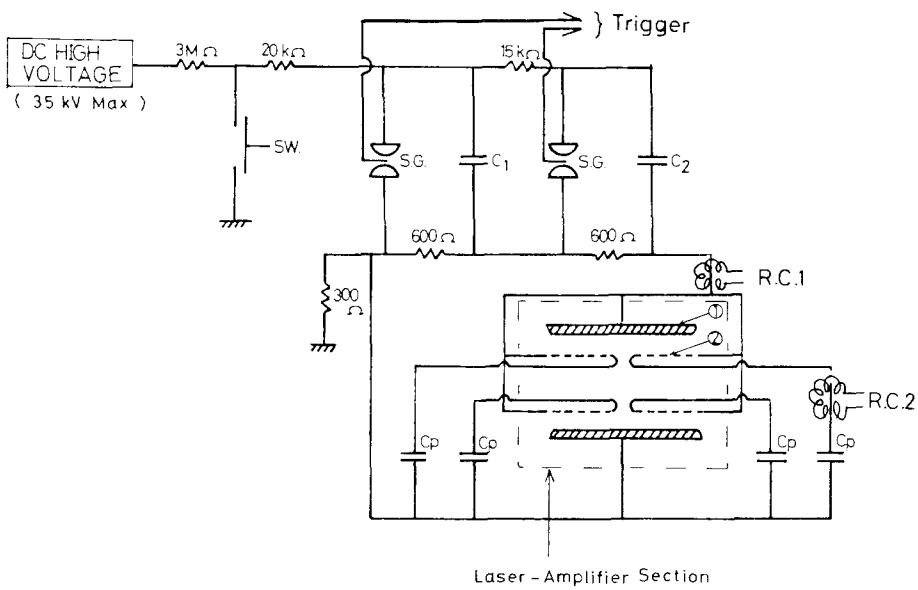

FIG. 3. Circuit diagram of the amplifier discharges; (1) main electrode (2) arc gaps for preionization, $C_{1,2} = 0.216$ μF (fixed), C_p variable.

Downloaded 13 May 2011 to 10.0.105.126. Redistribution subject to AIP license or copyright; see http://rsi.aip.org/about/rights_and_permissions

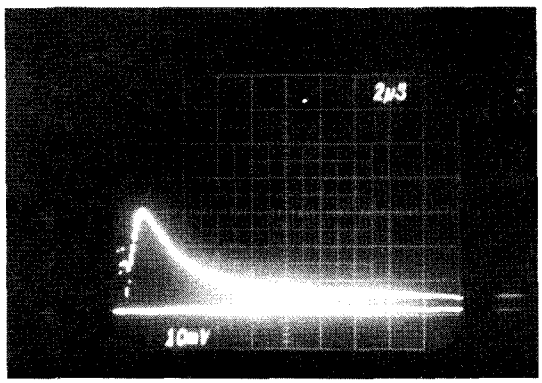

FIG. 5. A typical oscilloscope trace of the gain signal (time scale 2 μs/div.).

Fig. 7(b), the effect of relative concentration of CO_2 gas is given under the optimum condition of Fig. 7(a), and the gain value increases monotonically with increasing relative CO_2 concentration. In the region of higher CO_2 concentration ($\gtrsim 80\%$), the main discharges tend to become unstable (arcing). The peak gain versus charging voltage (V_c) is shown in Fig. 8, and no saturation takes place up to $V_c \sim 34$ kV which is the limit of the present power supply.

Finally, the amplification factor is measured by a photon-drag detector (General Radio-GR874) for different types of oscillator output pulse: (1) for a multilongitudinal mode normal pulse with the first peak duration (FWHM) of about 200 ns (where the low-pressure cw oscillator section in Fig. 1 is out of operation), and (2) for a nearly single longitudinal mode long pulse (of the order of μs; where both oscillator sections are in operation). The pulse waveform of the oscillator output for (1) and (2) above are shown in Figs. 9(a) and 9(b), respectively. The timing of the main discharge of the preamplifier concerned is adjusted so that the oscillator output pulse may reach the preamplifier at the instant when its small-signal gain attains the maximum.

In the case of (1) above (the multilongitudinal mode pulse), the value of the energy amplification factor deter-

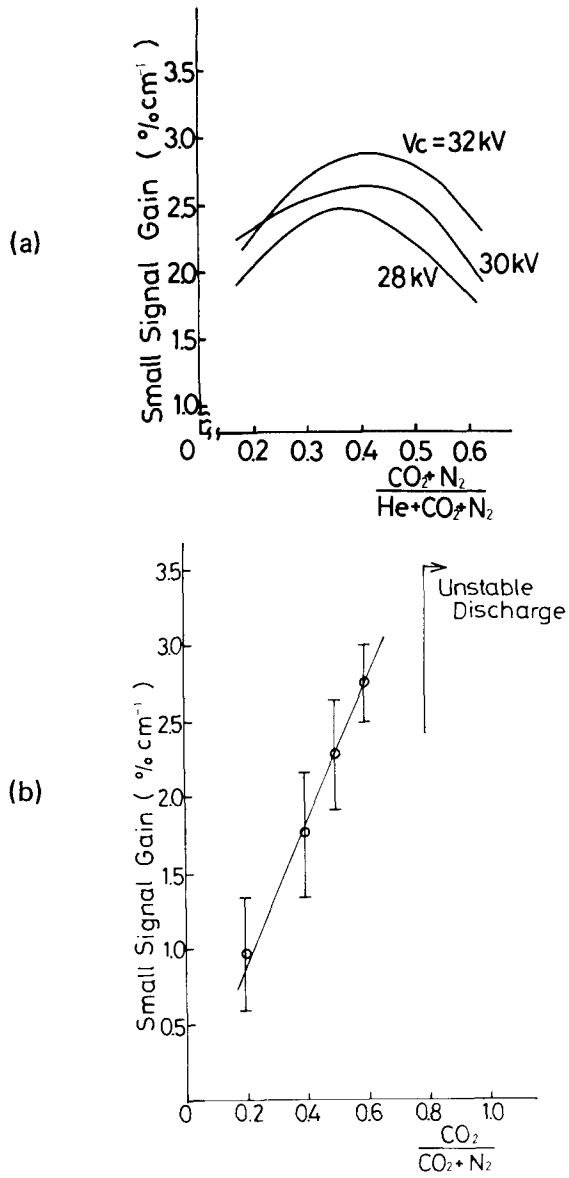

FIG. 7. Small-signal gain vs relative gas concentration ($d = 3.5$ cm, $4C_p = 9.6$ nF); (a) gain vs percentile CO_2 plus N_2, with CO_2:N_2 = 1:1, and (b) gain vs relative CO_2 concentration, with ($CO_2 + N_2$):He = 3:4; $V_c = 30$ kV.

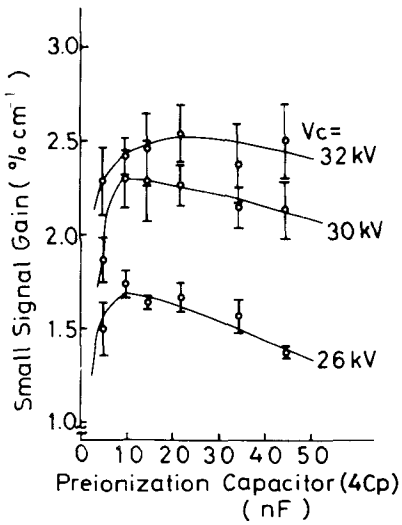

FIG. 6. The value of small-signal peak gain vs the capacitance of $4C_p$; $d = 3.5$ cm, CO_2:N_2:He = 3:3:8.

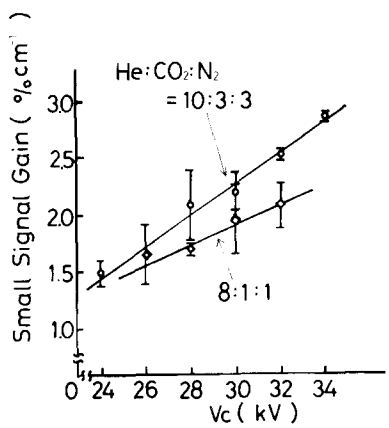

FIG. 8. Small-signal gain vs Marx charging voltage (V_c); $d = 3.5$ cm, CO_2:N_2:He = 3:3:10 and 1:1:8, $4C_p = 9.6$ nF.

Downloaded 13 May 2011 to 10.0.105.126. Redistribution subject to AIP license or copyright; see http://rsi.aip.org/about/rights_and_permissions

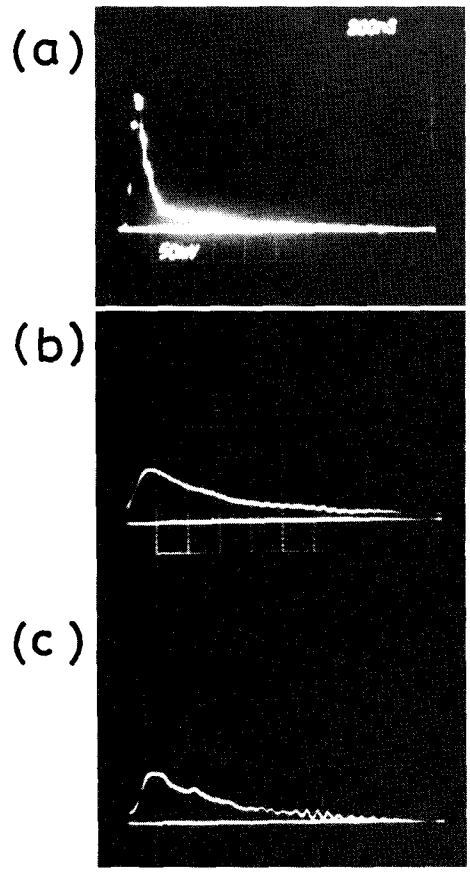

FIG. 9. Typical waveforms of long pulse; time scale 200 ns/div., (a) ordinary multilongitudinal mode amplifier input pulse, (b) single longitudinal mode long-pulse amplifier input pulse (20 mV/div.), and (c) amplifier output pulse corresponding to (b) (50 mV/div.); $d = 3.5$ cm, $V_c = 30$ kV, and CO_2:N_2:He = 3:3:10, $4C_p = 9.6$ nF.

mined is 4.7 for CO_2:N_2:He = 4.5:3:10, $V_c \sim 30$ kV, and $4C_p \sim 9.6$ nF at the input laser energy level of nearly 0.5 J. This means that the extraction energy from the active laser volume is approximately 14 J/l. In the case of (2) (the nearly single longitudinal mode long pulse), on the other hand, the corresponding value is about 3.8 for CO_2:N_2:He = 3:3:10, $V_c \sim 30$ kV, and $4C_p \sim 9.6$ nF at the input energy level of about 0.5 J (the extraction energy ~ 10 J/l). These amplification factors may increase further with increase of the charging voltage V_c. The preamplifier output waveform for case (2) is shown in Fig. 9(c), which demonstrates that a long laser pulse may be amplified without significantly enhanced distortion in the waveform. A minor fluctuation observed is probably due to the fact that the input laser beam is not completely single longitudinal mode.

III. DISCUSSION

In what follows, let us discuss the operating characteristics of the simplified preamplifier system proposed in this article. First, as seen in Fig. 4, the preionization current takes the form of a damped sinusoidal oscillation, whereas the main-discharge current exhibits a pulse shape of nearly half that period. The value of effective inductance (L_p) and resistance (R_p) of the preionization circuit are calculated from these observed waveforms to be $L_p \sim 0.3\ \mu$H and $R_p \simeq 0.6 \sim 1.2\ \Omega$, respectively; and the inductance of the main-discharge circuit (L_m) is $\sim 0.8\ \mu$H. Furthermore, it is generally known that the electrode voltage (V_d) in high-pressure glow discharge is kept nearly constant, independent of the discharge current.[8] The voltage is mainly determined by the total pressure and relative concentration of mixture gases as well as the electrode spacing. In addition, in the present experimental arrangement (Fig. 3), both the main-discharge current (i_m) and preionization current (i_p) rise simultaneously (Fig. 4). In view of such circumstances, the problem may be treated as that of a simple transient electric circuit as shown in Fig. 10. The circuit element C_m represents the total capacitance of the Marx generator ($C_m = 0.108\ \mu$F in the present experiment) and the others (L_m, L_p, C_p, and R_p) have already been defined in the above.

Thus, the problem is as follows: the switch (SW) is closed at $t = 0$ after the capacitor C_m is charged up to the voltage $V_m(t = 0) = 2V_c \equiv V_t$, where V_c is the Marx single stage voltage; and the currents $i_m(t)$ and $i_p(t)$ are solved for under the additional conditions that the main-discharge voltage V_d is kept constant irrespective of the value of main-discharge current, and the value of main-discharge current is approximately i_m since the peak value of i_m is greater than that of i_p by a factor of about 13. This simple electric circuit problem is easily solved, and the results read

$$i_m(t) = (C_m/L_m)^{1/2}(V_t - V_d)\sin \omega_m t \quad (\text{for } \omega_m t \lesssim \pi), \tag{1}$$

$$i_p(t) = 2(C_p/L_p)^{1/2} V_d\, e^{-t/\tau} \sin \omega_p t, \tag{2}$$

where

$$\omega_m = (L_m C_m)^{-1/2}, \quad \omega_p \sim [2(L_p C_p)^{1/2}]^{-1}, \quad \tau \sim 2L_p/R_p. \tag{3}$$

It is considered that the main-discharge current $i_m(t)$ becomes zero when the power source voltage $V_m(t)$ decreases to the value of V_d [Fig. 4(b) and Eq. (1)]. The peak value of i_m and i_p calculated from Eqs. (1) and (2) are shown in Figs. 11(a) and 11(b), respectively, for three assumed values of V_d. The values of circuit parameters required for computation are given above. The corresponding experimental values are also shown in the same figures by the dots with error bars. The comparison indicates that the calculated peak values of i_m and i_p agree well with the experimental ones when the V_d value, which is not exactly measurable, is

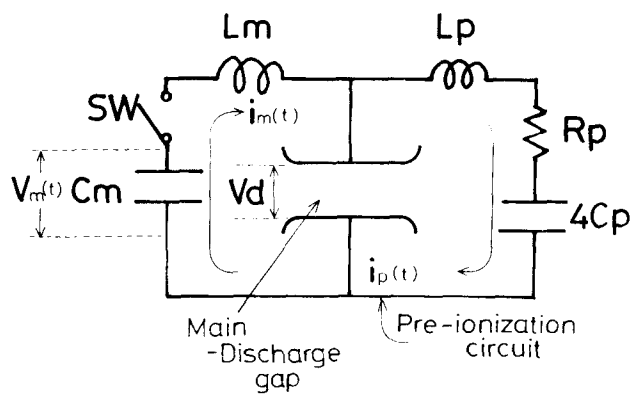

FIG. 10. Equivalent circuit; $C_m = 0.1$–$8\ \mu$F, $L_m \sim 0.8\ \mu$H, $L_p \sim 0.3\ \mu$H, and $4C_p$ is the total capacitance of the preionization-control capacitors (5–45 nF variable).

Downloaded 13 May 2011 to 10.0.105.126. Redistribution subject to AIP license or copyright; see http://rsi.aip.org/about/rights_and_permissions

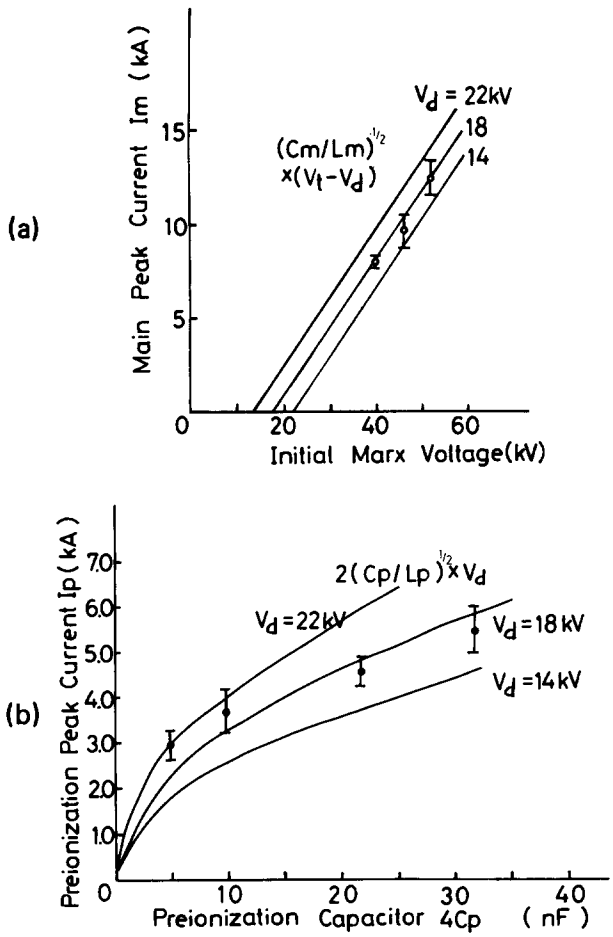

FIG. 11. Comparisons of the calculated peak discharge currents (i_m and i_p) with the corresponding measured values; (a) the peak values of i_m calculated from Eq. (1) vs $V_t = 2V_c$ and the corresponding measured values (the points with error bars), $4C_p = 9.6$ nF, and (b) the peak value of i_p calculated from Eq. (2) vs $4C_p$ and the corresponding measured values, $V_t = 2V_c = 52$ kV ($d = 3.5$ cm, CO_2:N_2:He = 3:3:8).

taken to be 18 kV in this example ($d = 2.5$ cm and CO_2:N_2:He = 3:3:8).

Reference 10, which describes an *oscillator* experiment with a similar size discharge chamber and bank energy, suggests that, in order to produce the laser output energy efficiently, the input energy for the UV preionizer is required to be in excess of 2% of the input energy for the main discharge. In the present experiment, the input energy for the UV preionizer in the case of 4 $C_p \sim 9.6$ nF (see Fig. 6, at which the small-signal gain nearly attains its maximum) is estimated to be 2% to 3% of that for the main discharge, and thus the result is consistent with that of Ref. 10. On the other hand, there also exist experimental observations[11,12] that the preionization level depends primarily on the peak value of the preionization discharge current. The peak current of preionization discharge in the present experiment is nearly 1 kA which is also nearly equal to the result of Ref. 10, where the input energy for the UV preionizer is 2% of that for main discharge. The extraction efficiency of this amplifier at $4C_p \sim 9.6$ nF, $V_c \sim 30$ kV is estimated to be 10%, which is slightly less than the oscillator lasing efficiency in Ref. 10 at similar conditions ($\sim 11\%$). This slightly lower extraction efficiency of the present amplifier could be attributed to the absence of timing control between the two discharges.

Next, let us discuss the reason for the existence of an optimum value of capacitance for preionization control. In the present arrangement, the total energy available in the Marx generator [equal to $(1/2)C_m V_t^2$] is divided into two parts: the main discharge and arc discharges for preionization. It may be intuitively understood that, if the C_p value is too small, the energy input to the preionization circuit is not enough to achieve adequate preionization,[9] so that the small-signal gain increases with increasing C_p in the region of smaller values of C_p. If the C_p value becomes too large, total energy injected into preionization prevails and that for the main-discharge decreases.

In order to confirm this, input energy density to the main discharges is considered. It is assumed that (1) an adequate preionization is provided, and (2) the excitation efficiency of population inversion for CO_2 lasing is unchanged for minor variation of the electric field in the interelectrode space. Then the small-signal gain (g) may be considered to be proportional to the input energy density to the main discharge, which may be written in the present case as

$$g \propto [(1/2)C_m(V_t^2 - V_d^2) - 2C_p V_d^2]/v, \tag{4}$$

where v is the effective volume of the main discharge, equal to the electrode area times the interelectrode spacing d; and $(1/2)C_m V_d^2$ is the energy remaining in the capacitor C_m when $V_m(t)$ has decreased to V_d and the main discharge has ceased. The quantity $(2C_p V_d^2)$ is the total energy consumed in the preionization circuit, which is equal to

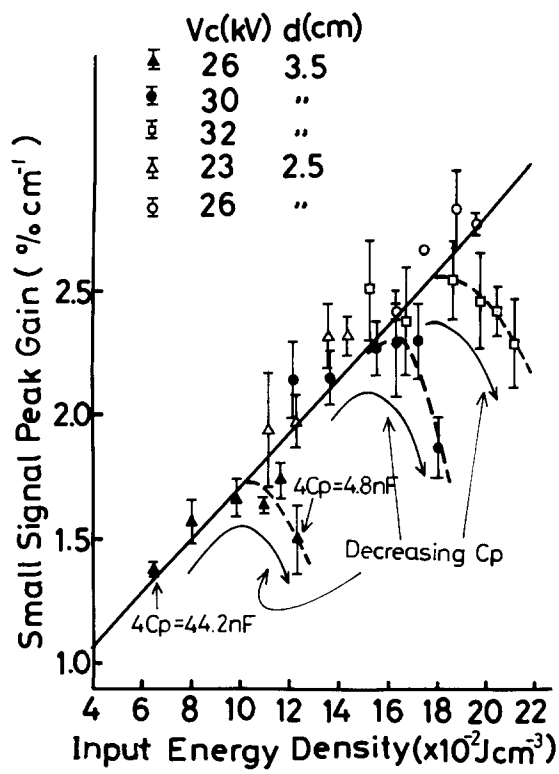

FIG. 12. Small-signal gain vs the input energy density to the main discharge calculated from Eq. (4). This is the redrawing from the experimental results such as shown in Fig. 6.

Downloaded 13 May 2011 to 10.0.105.126. Redistribution subject to AIP license or copyright; see http://rsi.aip.org/about/rights_and_permissions

$$\int_0^\infty i_p^2 R_p \, dt$$

and is calculated by using Eq. (2) under the condition $(\omega_p \tau)^2 \gg 1$.

The experimental results of small-signal gain vs $4C_p$, such as shown in Fig. 6, are summarized and redrawn in Fig. 12 for various values of $V_c (= V_t/2)$ and d. For each value of V_c, the value of $4C_p$ was varied from 44.2 to 4.8 nF. Here, the input energy density to the main discharge calculated from the right-hand side of Eq. (4) is taken as the abscissa, in place of the value of $4C_p$ in Fig. 6. In the calculations of Eq. (4), the value of V_d is 18 kV for $d = 2.5$ cm and 25 kV for $d = 3.5$ cm in this particular example of CO_2:N_2:He = 3:3:8.

The results of Fig. 12 indicate that the experimentally determined values of g are in fact nearly proportional to the input energy density, only if an adequate preionization is provided by employing the C_p value beyond a certain threshold. When the preionization becomes insufficient, with smaller values of C_p, the gain curves begin to deviate and decrease from the common straight line. Thus, there exists an optimum C_p value so as to maximize the gain value for a fixed combination of the V_d and d value. The optimum energy input to the preionization is found to be 2%–3% of the total stored energy in the Marx generator in the example of the present experiment, as has been mentioned before.

ACKNOWLEDGMENTS

The authors wish to express their sincere gratitude to Professor M. Katsurai, Y. Iida, Lu Qiaoqing, and other members of our laboratory for encouraging and supporting this work.

[1] P. P. Pearson and H. M. Lamberton, IEEE J. Quantum Electron. **QE-8**, 145 (1972).

[2] H. Seguin and J. Tulip, Appl. Phys. Lett. **21**, 414 (1972).

[3] M. C. Richardson, K. Leopold, and A. J. Alcock, IEEE J. Quantum Electron. **QE-9**, 934 (1973).

[4] C. A. Fenstermacher, M. J. Nutter, W. T. Leland, and K. Boyer, Appl. Phys. Lett. **20**, 56 (1972).

[5] For instance; A. Kitsunezaki, M. Tanimoto, and T. Sekiguchi, Phys. Fluids **17**, 1895 (1974); S. Kogoshi, K. N. Sato, and T. Sekiguchi, J. Phys. D **11**, 389 (1978); R. E. Pechacek, J. R. Greig, M. Raleigh, E. W. Koopman, and A. W. Desilva, Phys. Rev. Lett. **45**, 256 (1980); H. Saito, K. N. Sato, and T. Sekiguchi, IEEE Trans. Plasma Sci. **PS-9**, 199 (1981); A. C. Walker, S. Kogoshi, T. Stamatakis, W. Ward, and I. J. Spalding, J. Phys. D **14**, 1247 (1981).

[6] A. Gondhalekar, E. Holzhauer, and N. R. Heckenberg, Phys. Lett. A **46**, 229 (1973).

[7] Y. Hiraiwa, Graduation thesis, University of Tokyo, 1982.

[8] L. J. Denes and J. J. Lowke, Appl. Phys. Lett. **23**, 130 (1973).

[9] S. Suzuki, Y. Ishibashi, M. Obara, and T. Fujioka, Appl. Phys. Lett. **36**, 26 (1980).

[10] Shun-ichi Suzuki, Yuko Ishibashi, Minoru Obara, and Tomoo Fujioka, Rev. Sci. Instrum. **53**, 189 (1982).

[11] Herb J. Seguin, J. Tulip, and Don C. Mcken, IEEE Quantum Electron. **QE-10**, 311 (1974).

[12] Y. Ohwadano and T. Sekiguchi, Jpn. J. Appl. Phys. **19**, 1493 (1980).

Downloaded 13 May 2011 to 10.0.105.126. Redistribution subject to AIP license or copyright; see http://rsi.aip.org/about/rights_and_permissions